Solution Structure of Residues 1–28 of the Amyloid β-Peptide†

Joseph Talafous, Keith J. Marcinowski, Gilles Klopman, and Michael G. Zagorski*

Department of Chemistry, Case Western Reserve University, Cleveland, Ohio 44106

Received November 23, 1993; Revised Manuscript Received April 11, 1994®

ABSTRACT: The three-dimensional solution structure of residues 1–28 of the amyloid β-peptide was determined using nuclear magnetic resonance spectroscopy, distance geometry, and molecular dynamic techniques. The nuclear magnetic resonance data used to derive the structure consisted of nuclear Overhauser enhancements, vicinal coupling constants, and temperature coefficients of the amide-NH chemical shifts. The β-peptide is the major proteinaceous component of amyloid deposits in Alzheimer's disease. In membranelike media, the peptide folds to form a predominately α-helical structure with a bend centered at residue 12. The side chains of histidine-13 and lysine-16 are close, residing on the same face of the helix. Their proximity may constitute a binding motif with the heparan sulfate proteoglycans. The molecular details of the structure shown here could facilitate the design of rational treatments to curtail the binding of heparan sulfate proteoglycans or to prevent an α-helix→β-sheet conversion that may occur during the early stages of amyloid formation in Alzheimer's disease.

The most common cause of adult onset dementia is Alzheimer's disease (AD), now affecting approximately 12.5 and 47.2% of the population in the United States over the ages 65 and 85, respectively (Cotman et al., 1993). Patients with AD contain large quantities of insoluble amyloid plaques that are primarily found in brain tissue. A major component of amyloid plaque is the β-peptide (Glenner & Wong, 1984; Masters et al., 1985), a small (39–43 amino acids) polypeptide with heterogeneous termini that is generated from the cleavage (Golde et al., 1992; Sisodia, 1992) of a larger amyloid precursor protein (APP) (Figure 1). The major β-peptide component of amyloid plaque contains 42 amino acid residues (Roher et al., 1993) and is referred to as β-(1–42). The β-(1–28) and β-(29–42) peptides (Figure 1) occupy the extracellular and transmembrane regions of APP and β-(1–42).

Amyloid deposition is likely a critical step in the neurodegenerative processes associated with AD (Selkoe, 1991; Golde et al., 1992). Amyloid plaques are invariably associated with areas of nerve cell death, and the injection of synthetic β-peptides directly into rat brain produced cytotoxic effects (Kowall et al., 1991). In addition, a direct association exists between the aggregational state of β-peptide and neurotoxicity (Pike et al., 1993). It has also recently been established that soluble extracellular β-peptide is *normally* produced in cultured cells and human biological fluids (Shoji et al., 1992; Haass et al., 1992; Seubert et al., 1992; Busciglio et al., 1993). Therefore, it is now critically important to identify the factors that cause soluble, extracellular β-peptide to form the insoluble amyloid (Shoji et al., 1992), as well as to understand the mechanism of β-amyloidosis in AD (Seubert et al., 1992).

Recent work has also established that in membrane systems, such as planar lipid bilayers and solvent-free lipid bilayers, the β-peptide does not precipitate as amyloid, but instead produces voltage-dependent ion channels (Arispe et al., 1993a,b). In AD, a defect in the normal channeling of potassium and calcium (Etcheberrigaray et al., 1993) exists, together with a direct relationship between the aggregational state of β-peptide and the loss of calcium homeostasis (Mattson et al., 1993). It was speculated that such alterations in ion homeostasis, along with β-peptide deposition as amyloid, may both contribute to the neurodegenerative processes associated with AD.

In vitro studies (Barrow & Zagorski, 1991; Fraser et al., 1991; Hilbich et al., 1991; Burdick et al., 1992; Lansbury, 1992; Otvos et al., 1993) indicate that synthetic β-peptides can adopt either monomeric α-helical or oligomeric β-sheet conformations in solution. The α-helical conformation is very soluble, whereas the β-sheet conformation is less soluble and eventually precipitates as amyloid. The α-helical conformation is favored in membranelike conditions at high and low pH, while the β-sheet conformation is favored in water at midrange pH values (Figure 1). The variance in conformations is largely due to the 1–28 peptide region of β-peptide, since the β-(1–28) peptide can produce soluble monomeric α-helical structures (Barrow & Zagorski, 1991; Otvos et al., 1993), as well as plaquelike oligomeric β-sheet structures similar to those found in natural amyloid plaques (Kirschner et al., 1987; Gorevic et al., 1987). In contrast, the region composed of residues 29–42 is hydrophobic, is sparingly soluble, and aggregates into non-amyloid-like β-sheet structures (Halverson et al., 1990; Barrow & Zagorski, 1991; Hilbich et al., 1991; Barrow et al., 1992).

Nevertheless, a molecular basis for amyloid and channel formation remains undefined due to the lack of definitive structural data for the β-peptide. We report here a three-dimensional structure of the β-(1–28) peptide in solution. This structure represents the first high-resolution structural model of a β-peptide fragment and was derived using well-established two-dimensional (2D) NMR, molecular dynamics, and distance geometry techniques. Unlike the oligomeric β-pleated-sheet structure in amyloid plaques, the solution structure in membranelike media is almost entirely α-helical. The three-dimensional structure shown here will help to establish a molecular basis for amyloid formation, which may ultimately lead to the design of rational treatments to either block the β-peptide ion channels or curtail amyloid formation in AD.

† This work was supported by grants from the American Health Assistance Foundation (M.G.Z.) and the Suntory Institute for Bioorganic Research (M.G.Z.).

* Author to whom correspondence should be addressed.

® Abstract published in *Advance ACS Abstracts,* June 1, 1994.

0006-2960/94/0433-7788$04.50/0

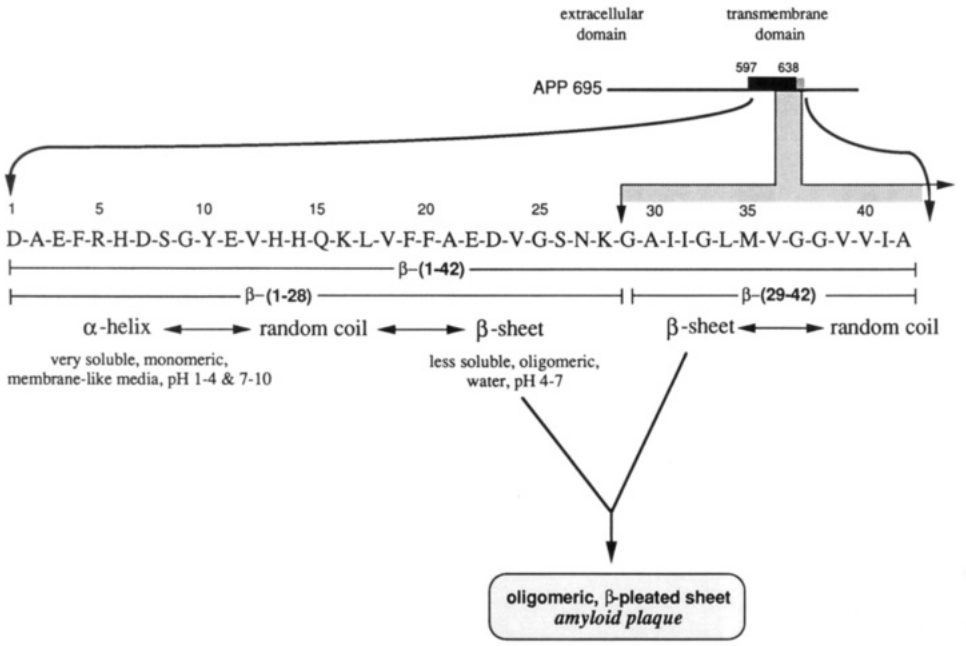

FIGURE 1: Overview of the formation of β-peptide from the amyloid precursor protein that contains 695 residues. The amino acid sequences of the β-peptides discussed in the text are also shown. This diagram emphasizes that, depending upon the conditions, residues 1–28 and 29–42 can exist in distinct conformations and aggregational states in solution. By contrast, in the amyloid deposit the β-peptide adopts an oligomeric β-pleated-sheet structure.

MATERIALS AND METHODS

Sample Preparation. The β-(1–28) peptide was synthesized, purified, and characterized as described previously (Barrow et al., 1992). Samples were prepared for NMR measurements by dissolving the peptide (3.6 mg, 0.001 mmol) in a solution (0.50 mL) containing either (1) perdeuterated sodium dodecyl sulfate (450 mM) in a mixture (by volume) of H_2O/D_2O (9:1) or (2) H_2O/trifluoroethanol-d_3 (4:6). The perdeuterated sodium dodecyl sulfate (SDS-d_{25}) and trifluoroethanol-d_3 (TFE-d_3) were purchased from Cambridge Isotopes, Inc. All solutions also contained 0.5 mM Na_2EDTA and 0.05 mM NaN_3. The pH of a solution was adjusted with a pH meter (Omega Engineering, Inc.) equipped with an electrode (Microelectrodes, Inc.) that fit inside the 5-mm NMR tube. The desired pH values were obtained at room temperature by adding microliter amounts of either dilute DCl or dilute NaOD. No corrections of pH readings were made for isotopic effects or for the presence of SDS-d_{25} or TFE-d_3, since control experiments showed that these substances did not significantly alter the pH.

Procedures for NMR Data Acquisition and Analysis. All proton (^1H) NMR spectra were obtained at 500 and 600 MHz using General Electric GN-500, Bruker AM-500, or Bruker AM-600 spectrometers. Two-dimensional NMR data were transferred to Indigo XS24 (Silicon Graphics, Inc.) computer workstations and processed using the FELIX program (version 2.05, Biosym, Inc.). Chemical shifts are referenced to internal sodium 3-(trimethylsilyl)propionate-*2,2,3,3-d*$_4$ (TSP). Probe temperatures were calibrated using dry methanol (Van Geet, 1970).

Two-dimensional nuclear Overhauser enhancement spectroscopy (NOESY) (Jeener et al., 1979) was run in the phase-sensitive mode with quadrature detection in both dimensions (States et al., 1982). The carrier was placed in the center of the spectrum at the position of the H_2O signal, and the H_2O signal was suppressed by irradiation with the proton decoupler. For the NOESY experiment, the irradiation was carried out during the recycle delay (which varied from 2.0 to 5.0 s) and during the mixing time (which varied from 25 to 200 ms). Reduction of coil lead pickup (Dykstra, 1987) was accomplished by modification of the pulse sequences to include $90°_{x,y,-x,-y}$ pulses for both preparation and detection (Zagorski, 1992). For spectral assignments, before Fourier transformation, spectra were multiplied by a Lorentzian-to-Gaussian weighting factor in F_2 and a 60–90°-phase-shifted sine bell in F_1. For quantitative measurements of NOE build-up rates, spectra were instead multiplied by a 90°-phase-shifted sine bell in both the F_2 and F_1 dimensions, as this avoided biasing peaks with narrower line widths. Baseline roll was reduced by careful adjustment of the intensity of the first points in F_2 and F_1 (Otting et al., 1986) and by the application of a cubic-polynomial baseline correction of the rows in the final 2D matrix. The spectral widths in both dimensions were ±2604 Hz, and a total of 512 increments (each consisting of 64–128 scans) was acquired with 2048 complex points for the F_1 and F_2 dimensions.

Distance Geometry and Simulated Annealing Computations. All computations and graphics visualizations were performed on Indigo XS24 (Silicon Graphics, Inc.) computer workstations using the programs X-PLOR (version 3.0; Brünger & Nilges, 1993) and INSIGHT II (Biosym, Inc.). The distance constraints were obtained from NOESY data by measuring NMR cross peak volumes with the FELIX program and were normalized for the number of atoms for a particular interaction. Of the 204 interresidue NOEs, 152 distance restraints (r_{ij}) were quantitatively derived from the cross-peak volumes (v_{ij}) of the NOESY spectrum with a mixing time (t_m) of 150 ms using the equation $r_{ij} = r_{kl}(v_{kl}/v_{ij})^{1/6}$, where k is the Hδ's of Tyr10, l is the Hε's of Tyr10, and r_{kl} was 2.49 Å. The final restraints employed were 1.8 Å as the lower bound and r_{ij} + 0.5 Å as the upper bound. The remaining 52 interresidue NOE cross-peaks were classified as medium (1.8–3.3 Å) or weak (1.8–5.0 Å) (Wüthrich, 1986). The 47 intraresidue distance restraints were obtained quantitatively from cross peaks in the NOESY spectrum (t_m = 150 ms) using the above equation, except that k and l were defined as the closest pair of atoms that formed a fixed distance. The

final intraresidue restraints employed were 1.8 Å as the lower bound and r_{ij} as the upper bound.

Our previous NMR data showed that the amide protons (NH's) for residues 5–27 were hydrogen bonded within an α-helical structure (Zagorski & Barrow, 1992). Using the NH temperature coefficients ($\Delta\delta/\Delta T$), the 23 hydrogen bonds were classified into three categories: 6 weak ($\Delta\delta/\Delta T \geq 8.0$), 9 medium ($8.0 < \Delta\delta/\Delta T \geq 5.0$), and 8 strong ($\Delta\delta/\Delta T < 5.0$). On the basis of these categories, the distances between the nitrogen of residue i and the carbonyl oxygen of residue $i-4$ were restrained to 2.3–3.2 Å for the weak, 2.5–3.2 Å for the medium, and 2.6–3.2 Å for the strong bond. The distance restraint between the NH of residue i and the carbonyl oxygen of residue $i-4$ was 1.6–2.2 Å for all three categories of hydrogen bonds. This procedure kept the angles closer to ideality for the stronger hydrogen bonds. Repeating the X-PLOR distance geometry/simulated annealing (DGSA) computations without the inclusion of any hydrogen bonds produced an essentially identical backbone structure within residues 9–28.

The vicinal coupling constants (J) were separated into three categories on the basis of their magnitudes (Zagorski & Barrow, 1992): small, 3–5 Hz; medium, 6–7 Hz; and large, 8–10 Hz. The three J categories were then converted into torsion angles with the following error limits: ±30° for small J, ±40° for medium J, and ±50° for large J (Wüthrich, 1986). The harmonic force constant was 10 kcal mol^{-1} rad^{-2}. Using the above restraints, the DGSA protocol was applied by the X-PLOR program. The 100 initial structures generated with metric matrix distance geometry were then subjected to molecular dynamics. For each structure, this involved an initial temperature of 3000 K, 5000 heating steps, 5000 cooling steps, and 2000 steps of Powell energy minimization. The time step was 0.003 ps, and the dielectric constant was 30. The remaining parameters employed in this study are described in the DGSA protocol in the manual supplied with X-PLOR.

RESULTS

NMR Measurements. We previously reported a complete ^{1}H NMR assignment of the β-(1–28) peptide dissolved in aqueous TFE-d_3 solution using standard 2D NMR techniques and sequential assignment procedures (Zagorski & Barrow, 1992). Using similar methods, the complete ^{1}H NMR assignment of the β-(1–28) peptide in SDS-d_{25} solution was obtained to elucidate its structure when micelle-bound. This approach, which adequately mimics the molecular environment of biological membranes, has been successfully applied to many polypeptides (McDonnell & Opella, 1993). To form uniform micelles and ensure that the β-(1–28) peptide was indeed micelle-bound, we used a relatively high concentration of SDS-d_{25} (450 mM), which is well above its critical micelle concentration of 8 mM (McDonnell & Opella, 1993). A more complete description of the effects of different micelle concentrations on the secondary structure of the β-peptide will be presented in a forthcoming publication.

The expanded region of the 2D NOESY spectrum shown in Figure 2 demonstrates that numerous, close (2.4–3.6 Å), through-space interactions or nuclear Overhauser effects (NOEs) are present between neighboring NH protons. This particular type of NOE [NN(i,i+1)], together with other weak-sized αN(i,i+1) NOEs and medium-sized αN(i,i+2), αN(i,i+3), αN(i,i+4), and $\alpha\beta$(i,i+3) NOEs observed in other spectral regions, establishes that the peptide exists in a well-defined α-helical conformation (Wüthrich, 1986). The presence of αN(i,i+4) NOEs indicates that a 3_{10}-helix is not

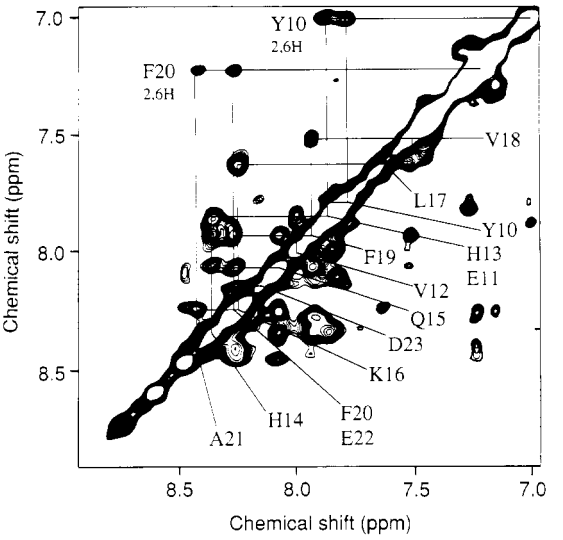

FIGURE 2: Portion of a NOESY contour plot of the amide–amide (NH–NH) region. The NH(i) to NH(i+1) through-space interactions from Tyr10 to Asp23 are shown with the NH assignments along the diagonal. NOEs from the aromatic 2,6H's of Tyr10 to the NH's of Tyr10 and Glu11, together with NOEs from the aromatic 2,6H's of Phe20 to the NH's of Phe20 and Ala21, are shown at the top of the plot. Spectra were recorded at 500 MHz using a 2 mM sample of β-(1–28) and a 450 mM sample of SDS-d_{25} dissolved in water (9:1, H_2O/D_2O) at pH 3.0 and 25.0 °C.

present. In addition, no alteration in the intensity of the majority of the NOEs was seen upon raising the temperature from 25 to 50 °C. This demonstrates that the α-helix is stable and free from rapid conformational averaging. Essentially identical NOE and circular dichroism data (CD) were observed in aqueous solutions containing either SDS or TFE (Barrow & Zagorski, 1991; Zagorski & Barrow, 1992), indicating that the β-(1–28) peptide adopts similar α-helical structures under both solution conditions.

Three-Dimensional Structures. The three-dimensional structure of the α-helical conformation was determined using the NMR data and the well-established DGSA protocol (Nilges et al., 1988; Brünger & Nilges, 1993). The NMR data consisted of 251 NOEs, 23 hydrogen bonds, and 27 dihedral angle constraints. Of the 251 NOEs, 204 were interresidue and 47 were intraresidue. NOE build-up rates obtained from NOESY data, acquired with mixing times of 25, 50, 100, 150, and 200 ms and a relaxation delay of 4.3 s, showed that spin diffusion was negligible (Wüthrich, 1986). Initially, 100 structures were generated by DGSA, of which 95 possessed very similar conformations and energies, demonstrating a high degree of convergence to a single family of structures (Figure 3, top). The remaining five structures were significantly strained, conformationally different, and discarded by the X-PLOR ACCEPT procedure. All accepted structures were close to ideal geometry and had no distance restraint violation greater than 0.3 Å (Table 1). The averaged structure, which was obtained from the 95 accepted structures and minimized with the restraints, had a low mean X-PLOR potential energy of 8.1 kcal mol^{-1} (Table 1). This demonstrates that virtually no strain was induced by the restraints.

Evaluation of the Structure with Respect to the NMR Constraints. The structure consists of two right-handed α-helices (residues 2–11 and 13–27), which are connected by a bend centered at Val12. The bend is consistent with the observed periodic nature of the αH chemical shifts (Blanco et al., 1992) and also with the NMR-derived NH temperature coefficients. A complete analysis of the NH, αH, and βH chemical shifts in water, water/TFE, and water/SDS will be

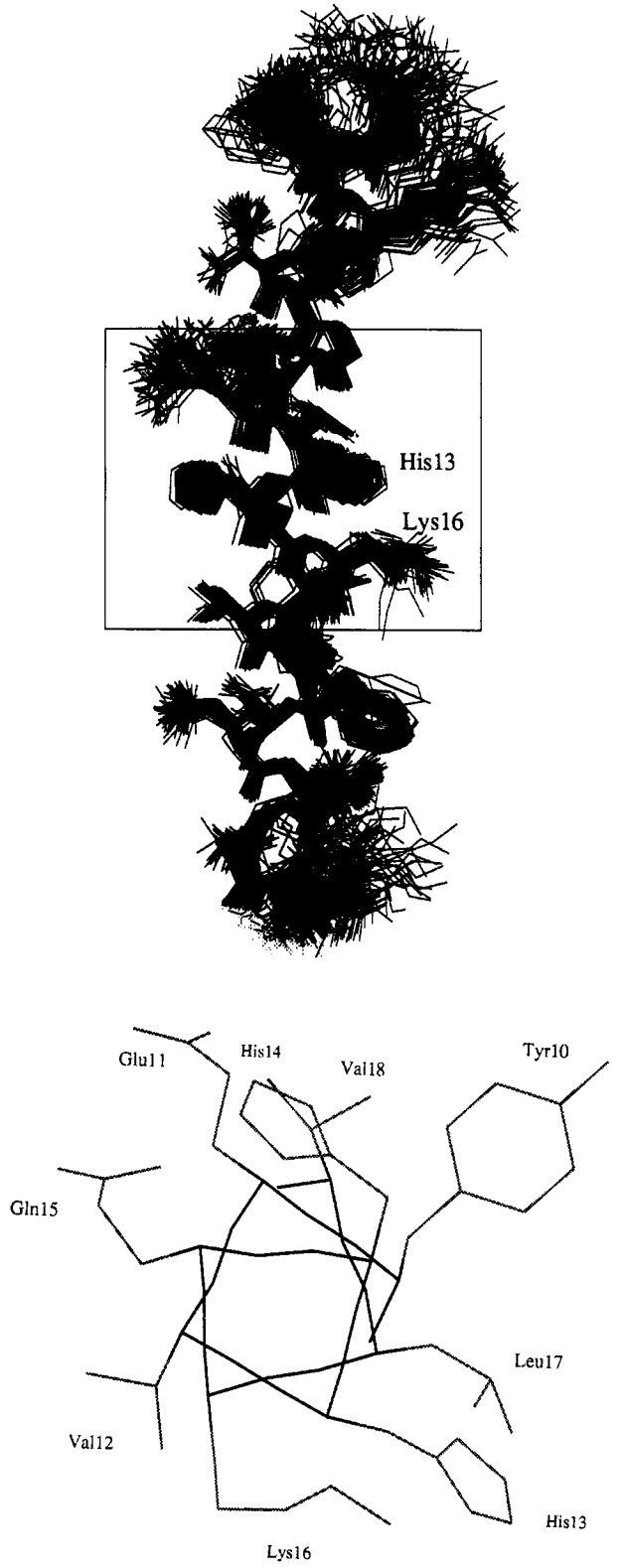

FIGURE 3: (Top) Final 95 structures of the β-(1–28) peptide superpositioned using the backbone atoms. The N-terminus is shown at the top and the C-terminus is shown at the bottom. The side chains of His13 and Lys16 are labeled to illustrate their proximity. (Bottom) An expanded view is shown along the helical axis between Tyr10 and Val18. This segment, which corresponds to the region within the box of the upper structures, is part of an averaged and minimized structure that was generated from the 95 structures. The ζ-NH_3^+ of Lys16 is solvent exposed, consistent with the NMR data (Zagorski & Barrow, 1992).

presented in a subsequent report. Repeating the DGSA computations without the hydrogen bond restraints produced an essentially identical bent α-helical backbone structure, so

Table 1: Structural Parameters and rmsd Values for the 95 β-(1–28) Structures[a]

rmsd from experimental restraints[b]	SA	$\langle SA \rangle_{r1}$
distance restraints (Å)		
interresidue (204)	0.044 ± 0.002	0.027
intraresidue (47)	0.090 ± 0.002	0.082
hydrogen bonds (46)	0.012 ± 0.007	
total (297)	0.052 ± 0.001	0.040
torsion angle restraints (deg)		
$\phi(27) + \chi(2)$	0.016 ± 0.002	1.160

X-PLOR potential energies (kcal mol^{-1})[c]	SA	$\langle SA \rangle_{r1}$	$\langle SA \rangle_{r2}$
bond	5.3 ● 0.3	2.5	0.6
angle	15.1 ± 1.2	4.8	0.1
improper	3.4 ± 0.4	0.8	0.5
total	23.8 ± 1.8	8.1	0.6

rmsd from idealized geometry	SA	$\langle SA \rangle_{r1}$	$\langle SA \rangle_{r2}$
bonds (Å)	0.005 ± 0.000	0.003	0.001
angles (deg)	0.56 ± 0.02	0.31	0.10
dihedrals (deg)	34.1 ± 1.6	35.2	35.0
impropers (deg)	0.45 ± 0.03	0.22	0.04

rmsd of coordinates (Å)	backbone	non-hydrogens
pairwise[d] of SA	0.69 ± 0.24	1.47 ● 0.27
SA vs $\langle SA \rangle$	0.48	1.04
$\langle SA \rangle$ vs $\langle SA \rangle_{r1}$	1.25	1.98
$\langle SA \rangle_{r1}$ vs $\langle SA \rangle_{r2}$	0.12	0.15

[a] rmsd represents the root-mean-squared deviation. SA is the family of 95 accepted structures resulting from the X-PLOR/DGSA procedure, $\langle SA \rangle_{r1}$ is the averaged family structure minimized with distance and torsion restraints applied, and $\langle SA \rangle_{r2}$ is $\langle SA \rangle_{r1}$ minimized without distance and torsion restraints. [b] All structures in SA had distance violations of less than 0.3 Å. [c] The van der Waals and electric potential energies were zero within the experimental errors. [d] rmsd was calculated between distinct pairs in SA and ranged from 0.18 to 1.99 for the backbone atoms and from 0.72 to 2.80 for the non-hydrogen atoms.

the bend alone is not a computational artifact of differences in hydrogen bond strengths.

The bend is consistent with the weak-sized αN(i,i+2) NOEs from Val12 to His14, from Val18 to Phe20, and from differences in other NOE intensities along this region of the peptide. The temperature dependence of the NH chemical shifts showed a weak NH bond for Val12 and a cluster of strong NH bonds within the His13-His14-Gln15-Lys16-Leu17 segment, whereas the next four residues (Val18-Phe19-Phe20-Ala21) have weaker hydrogen bonds. The latter four residues may also act as a hydrophobic shield to the NH protons of His13–Leu17 (Dyson & Wright, 1993). These data, together with several side-chain NOEs among Leu17, Phe20, and Val24, suggest that a slight packing of the hydrophobic residues occurs, in accordance with the observed bend of the helix.

Several of the measured J coupling constants between the NH and αH protons (Zagorski & Barrow, 1992) indicate that the helical structure may be in rapid equilibrium with an extended chain structure. Although the majority of the residues have J values of less than 6 Hz, only Val12, Phe19, and Phe20 have values under 4 Hz that are normally associated with rigid helical backbone structures (Pardi et al., 1984). The J values greater than 6 Hz are mostly found at the ends of the molecule, where more deviation from helicity is to be expected due to increased mobility or possible fraying. However, the relevance of the J coupling constants to the structure may be dubious, since J coupling constants usually

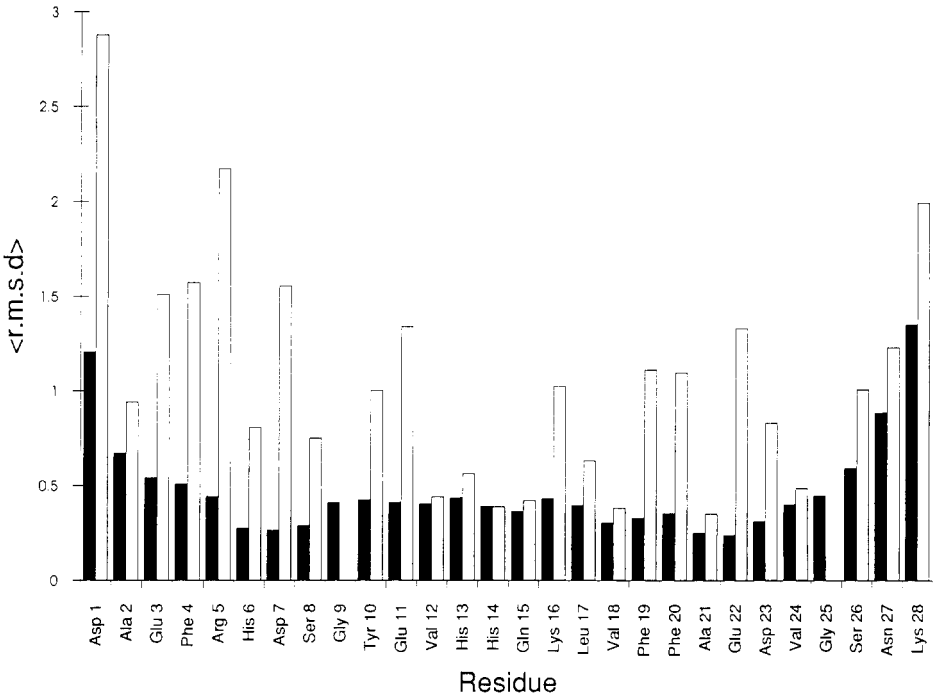

FIGURE 4: Average rmsd between the final 95 energy-minimized structures and the averaged/minimized structure of the β-(1–28) peptide. Two values are given for each residue: (1) the backbone C, Cα, N, and O subset of atoms (filled bars) and (2) the side-chain atoms (open bars). The rmsd values were determined using the modified AVERAGE procedure within the program X-PLOR.

are one of the least sensitive NMR parameters for the detection of folded conformations in flexible linear peptides (Dyson & Wright, 1991). Large populations of helical structure in peptides can have J values of 6–7 Hz. Moreover, a recent report established that J coupling constants can be inaccurate and that discrepancies occur between those measured from 2D DQF-COSY and resolution-enhanced 1D spectra (Merutka et al., 1993). To compensate for the possible J value errors in the structure computations, a reduced force constant of 10, rather than a more standard value of 50, was used for the 27 ϕ/ψ backbone dihedral angle constraints.

The NOE data obtained at 50 °C were very similar to the data seen at 25 °C, demonstrating that the β-peptide adopts an ordered α-helical backbone structure that is not subject to conformational averaging. This is supported by the observation of numerous medium-range $\alpha N(i,i+2)$, $\alpha N(i,i+3)$, $\alpha N(i,i+4)$, and $\alpha\beta(i,i+3)$ NOEs, together with the small temperature coefficients (less than 5). In addition, the majority of the αH proton chemical shifts are upfield relative to random coil values (Zagorski & Barrow, 1992), indicating helical structure (Szilágyi & Jardetzky, 1989; Wishart et al., 1991).

For the mean atomic positions of the 95 structures, the root-mean-squared deviation (rmsd) is 0.48 for all backbone atoms and 1.04 for all non-hydrogen atoms. Residues 4–25 are the most defined, with a backbone rmsd of 0.41 and a non-hydrogen atom rmsd of 0.86 (Figure 4). The side chains of the majority of the residues are also well defined, particularly in the middle region of the peptide (residues 12–24) except for Lys16. This high degree of structural definition can be rationalized by the numerous NMR restraints (greater than 15 restraints per residue), including stereospecific assignments of the prochiral pairs of protons. The three valine residues (Val12, Val18, and Val24) have rmsd values below 0.5, and all exist in a trans configuration, in accordance with the coupling constant and intraresidue NOE data. Val12, Val18, and Val24 displayed large vicinal coupling constants (11.2, 11.8, and 9.6 Hz) between the α- and β-protons (Zagorski & Barrow, 1992). Except for Val18, in which both γ-CH_3 groups are chemical shift equivalent, all valine residues showed separate strong and weak NOEs from each NH to each γ-CH_3. The side chains of His13, His14, and Gln15 likewise adopted unique and well-defined conformations with rmsd values less than 0.45 (Figure 4). The Gln15 side chain displayed separate weak- and medium-sized intraresidue NOEs from each ε-NH_2 proton to each γ-CH_2 proton. The Leu17 δ-CH_3 group had NOEs to the aromatic 2H of the His13 and the 4H of His14; also, the Val18 γ-CH_3 groups displayed NOEs to both the 2H and 4H of His14.

By contrast, the side chains of Arg5, Lys16, and Lys28 do not adopt distinct conformations, with somewhat higher rmsd values of 2.2, 1.1, and 2.1, respectively. This weaker definition results from the lack of NOE distance restraints. The lack of NOE data observed at the termini, notably, Asp1, Asn27, and Lys28, also causes substantially high side-chain rmsd values in the range 1.2–2.9 (Figure 4). This may be caused by fraying at the ends of the peptide, causing the apparent disorder seen in the overlaid structures (Figure 3, top).

DISCUSSION

Physiological Relevance of the Solution Conditions. The objective of this study was to determine the membrane-mediated structure of the β-(1–28) peptide using 2D NMR data. Difficulties with high-resolution NMR studies of peptide conformations in membranes arise from line broadening due to the high molecular weight of the peptide–membrane aggregates. A useful alternative is to select an organic solvent or micellar system in which the conformation of the peptide would resemble that of the membrane. SDS micelles have been reported to adequately mimic the membrane environment of membranes (Wu & Yang, 1981; Parker & Song, 1992; McDonnell & Opella, 1993). In addition, TFE is a membrane-mimicking solvent that promotes either inter- or intramolecular hydrogen bonding, analogous to SDS micelles or phospholipid vesicles, and stabilizes α-helices and β-sheets that are in

equilibrium with random coil structures (Nelson & Kallenbach, 1986). Studies using CD and NMR established that the propensity for helix formation in a peptide is a prerequisite for the induction of an ordered helix by TFE; thus, TFE will only stabilize (not induce) helical structures in peptide segments that have the propensity to do so based on their amino acid sequences (Dyson et al., 1992a,b). Similar conclusions were reached by others (Segawa et al., 1991; Sönnichsen et al., 1992), where only those peptide segments that correspond to helical segments in the native protein (as determined by X-ray diffraction in the solid state) adopt helical structure in TFE/water solutions. A potential pitfall is that TFE and SDS may provide an environment in which the β-peptide adopts a non-native conformation. On the other hand, when used as cosolvents with water, these solvents may mimic a more natural and realistic environment that exists for a given peptide in vivo, such as that found in lipid/water interfaces. For instance, for the peptide gastrin, the degree of secondary structure in TFE/water solutions correlated well with its biological potency (Mammi et al., 1988).

Many studies indicate that only amphiphilic peptides form helical structure in SDS solution (Parker & Song, 1992). Thus, because the β-(1–28) peptide is not amphiphilic, the observation of helical structure in SDS solution may be exceptional. The β-(29–42) peptide (Barrow et al., 1992) adopts either a β-sheet or random coil structure rather than an α-helical structure in TFE and SDS solutions (M. G. Zagorski, unpublished result), and similar conclusions were obtained with other peptides [see Waterhous and Johnson (1994) and references cited therein].

Numerous reports have revealed membranelike components in preamyloid deposits (Yamaguchi et al., 1990; Masliah et al., 1991; Namba et al., 1991). Additionally, there are extensive experimental data which suggest that alterations of membrane integrity in brain cells and endothelial cells occur in AD, and many reports have correlated these changes to the occurrence of amyloid deposits (Mancardi et al., 1980; Barany et al., 1985; Zubenko et al., 1987; Pettegrew et al., 1988; Blusztajn et al., 1990; Nitsch et al., 1992). Thus, our rationale for NMR studies in membranelike environments is that the β-peptide exists in membranelike compartments within preamyloid deposits, and the β-peptide is found on the basement membrane of cerebral blood vessels, which are sites for the early stages of amyloid deposition (Miyakawa et al., 1982). Residues 8–17 of β-peptide can associate and bind to lipid receptors (Allsop et al., 1988); also, the 29–42 segment should interact favorably with lipids or membranes, as this segment is hydrophobic and naturally membrane-bound in APP (Figure 1).

Relationship between the Biological Activities and the Structures of β-Peptide. Although the biological role of the amyloid β-peptide has yet to be determined, it is thought to contribute to the progressive neuronal loss of AD. The introduction of purified β-peptide from amyloid plaque cores causes focal neuronal damage (Frautschy et al., 1991), and the injection of synthetic β-(1–40) peptide into rat brain resulted in β-amyloid deposits with surrounding nerve cell degeneration (Kowall et al., 1991). However, regarding the neurotoxicity tests, considerable discrepancies exist across different laboratories [for a review, see *Neurobiology of Aging* (1992) *31*, 535–623]. Several groups have reported that synthetic β-peptides show either trophic or toxic responses on neurons in vitro. The reasons for these deviations are unknown, although they are believed to arise in part from differences in the aggregation states and the solution structures of the β-peptides.

It was recently established that for the β-(1–40) peptide the random coil structure is nontoxic, while the β-sheet structure is neurotoxic (Simmons et al., 1993). In addition, the amount of β-sheet structure correlated with the levels of neurotoxicity. Over time, in aqueous solution, the β-(1–40) and β-(1–42) peptides adopt greater amounts of oligomeric β-sheet structure (Barrow & Zagorski, 1991; Fraser et al., 1991; Barrow et al., 1992), and these results are consistent with the ability of "aged" or aggregated β-peptide to be neurotoxic and "fresh" or monomeric β-peptide to be nontoxic and enhance neurite outgrowth (Pike et al., 1991, 1993). Interestingly, if the aggregation process is reversed by dissolving aged β-(1–42) in hexafluoroisopropyl alcohol, which promotes α-helical structure for residues 1–28 and random coil structure for residues 29–42 (Barrow et al., 1992), the neurotoxicity disappears (Pike et al., 1993). One possibility is that the monomeric α-helical conformation is the neurotrophic species, and when an α-helix (monomeric)→β-sheet (oligomeric) transformation occurs, the β-peptide becomes neurotoxic. To evaluate this hypothesis, additional studies examining the effects of the α-helical structure on nerve cell cultures are required.

General Features of the Structure. Overall, the three-dimensional structure of the β-(1–28) peptide consists of a bent α-helix with the bend centered at Val12. Except for the disorder at the termini (Figure 3, top), the 95 computed structures showed a high degree of convergence with relatively low rmsd values (Figure 4). This high degree of structural definition results from the large ensemble of NMR constraints, which included at least 15 restraints per residue for the region between residues 4 and 25. It should be kept in mind that a low rmsd does not mean a small conformational space was sampled for the peptide in solution, but rather establishes that a high degree of precision was obtained for the solution coordinates (Powers et al., 1993). To examine these possibilities, additional NMR relaxation time studies using ^{13}C- and ^{15}N-enriched β-peptides are being performed to compare the dynamics and local mobilities in different regions of the peptide.

The helical structure is consistent with the NMR data, except for some of the *J* coupling constants between the αH and NH protons. An identical three-dimensional structure was obtained using a different protocol, which included the distance geometry algorithm implemented in the program DGII (Havel, 1991) as part of the INSIGHT II software package (Biosym, Inc.). This result establishes that the structures shown here are not biased by computational methods.

Homologies with Other Curved α-Helical and Ion-Channel-Forming Peptides. The β-(1–40) peptide produces cation-selective channels in bilayer membranes (Arispe et al., 1993a,b). Recent 2D NMR studies of the β-(1–39) peptide in TFE solution demonstrated that residues 1–28 are helical and residues 29–39 are disordered (M. G. Zagorski et al., unpublished result). This latter interpretation is consistent with CD data, in which the β-(29–42) peptide is primarily random coil in TFE solution and the β-(1–39) and β-(1–28) peptides adopt 45% and 65% α-helix structure, respectively (Barrow et al., 1992). These results suggest that, in TFE solution and perhaps in bilayer membranelike solutions similar to SDS, the same residues adopt α-helical conformations in both peptides.

We compared the structure of the β-(1–28) peptide to the structures of alamethicin and melittin, which are small peptides that likewise form ion channels in bilayer membranes (Sansom, 1991). Superposition of the backbone conformation of the β-(1–28) peptide with the X-ray crystallographic backbone structures of alamethicin (Fox & Richards, 1982) and melittin (Terwilliger & Eisenberg, 1982) revealed that, despite the lack of any obvious sequence homology, the backbone tertiary structures of these three peptides are very similar, particularly in the degree of helical bending. The rmsd between residues 2–21 of alamethicin and 1–20 of mellitin is 1.84 Å; the rmsd of regions 1–20 of the β-(1–28) peptide to alamethicin and melittin are 1.74 and 1.47 Å, respectively. In solution or in the crystalline state (Terwilliger & Eisenberg, 1982; Bazzo et al., 1988; Ikura et al., 1991), melittin folds to form two α-helices joined by a bend between Thr11 and Gly12. The β-(1–28) peptide has a helix–helix angle of 21°, which is almost identical to the 20° value for melittin in methanol solution (Bazzo et al., 1988). This angle was determined by a least-squares fit between the β-(1–28) peptide and two appropriately sized ideal right-handed α-helices.

The bend in the β-(1–28) peptide cannot be ascribed to amphipathicity, nor to the absence of a hydrogen bond. Many α-helical segments in proteins are curved, bent, or kinked (Barlow & Thornton, 1988). The bends are usually amphipathic or associated with a proline residue, as in the case of melittin and alamethicin. The amphipathicity generally causes a bend by allowing the hydrophobic face to be concave and the hydrophilic face to be convex, with the centrally located proline promoting helix bending by the absence of a hydrogen bond.

The β-(1–28) peptide, alamethicin, and melittin likewise share several biophysical properties. First, the β-peptide and melittin both induce lipid phase separation and decrease the fluidity of membranes (Chauhan et al., 1993). Second, replacement of Pro14 in melittin dramatically alters its channel-forming properties (Sansom, 1991; Dempsey, 1990). By analogy, amino acid substitutions near the bend region of the β-peptide may also destroy its channel activity. For example, substitution of the His13–His14 segment in β-peptide promotes its precipitation as a β-pleated-sheet structure (Hilbich et al., 1991). Thus, the bend may be important for the stabilization of the α-helical structure, as well as for ion channel activity. The third similarity is a β-sheet→α-helix conversion, which occurs for β-peptide (Barrow & Zagorski, 1991; Zagorski & Barrow, 1992) and was proposed to occur within the alamethicin ion channel (Hall et al., 1984). Given the wealth of information concerning both the structural and functional properties of alamethicin and melittin (Sansom, 1991), these peptides provide good starting points in designing models of ion channel formation in β-peptide.

Binding Motif of Proteoglycans and Other Proteins. Binding of the β-peptide to the highly negatively charged heparan sulfate proteoglycans (HSPG) enhances the aggregation of β-peptide (Snow et al., 1991). On the basis of comparisons with consensus sequences from other known HSPG-binding proteins, the Val12-His13-His14-Gln15-Lys16-Leu17 segment was identified as a likely site for binding with HSPG (Fraser et al., 1992). Regarding the α-helical structure, we note that the side chains of His13 and Lys16 are proximate and reside on the same face of the molecule (Figure 3b). Both His13 and Lys16 are important residues for amyloid fibril production (Fraser et al., 1991; Kirschner et al., 1987), and rodents with the His13→Arg mutation do not develop mature amyloid deposits (Johnstone et al., 1991). Recent

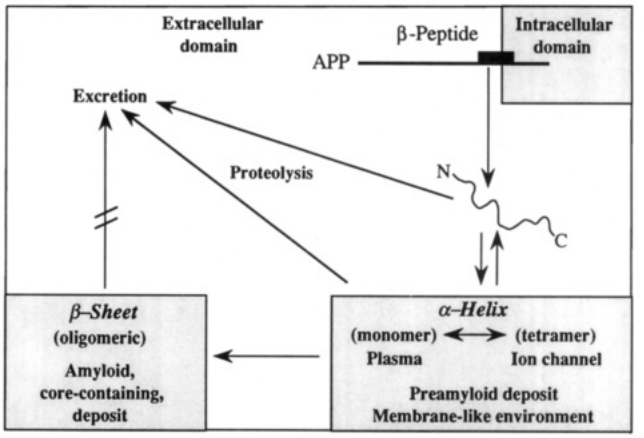

FIGURE 5: Scheme for the fate of β-peptide after being generated by the proteolysis of APP and eventually precipitating as amyloid in a β-sheet structure. This updated scheme, based upon our earlier version (Barrow et al., 1992), now incorporates more recent results about the ability of β-peptide (1) to exist normally in soluble forms (Shoji et al., 1992; Haass et al., 1992; Seubert et al., 1992; Busciglio et al., 1993) and (2) to produce ion channels in membranelike media (Arispe et al., 1993a). On the basis of the present results, we propose that the β-peptide ion channel consists of a tetrameric α-helical structure.

data from our laboratories showed that the addition of heparin to a solution of the β-(1–28) peptide causes the 2H and 4H NMR signals of His13 to shift and broaden (Keane & Zagorski, unpublished result). This result, together with the proximal location of His13 and Lys16, is consistent with the proposition that these residues may constitute a binding motif with glycosaminoglycans (Snow et al., 1991; Fraser et al., 1992; Brunden et al., 1993). In fact, an analogous structural motif may be involved in the binding of the β-peptide to transthyretin, a normal protein component of plasma (Schwarzman et al., 1994). A structural model for the complex of transthyretin and the α-helical structure of the β-peptide showed that the side chains of His13 and Lys16 form part of a positive potential binding surface that makes contact with a negative potential surface of transthyretin.

Fate of β-Peptide In Vivo. Outlined in Figure 5 is a hypothetical scheme that correlates the various biological activities with the different structures of β-peptide. This scheme is based on our previous work and now incorporates the results of the present study. In our original work, we proposed that the β-peptide may normally exist in human biological fluids in a soluble form (Barrow & Zagorski, 1991). Subsequently, this proposition was supported using both in vivo and in vitro studies (Shoji et al., 1992; Haass et al., 1992; Seubert et al., 1992; Busciglio et al., 1993).

Once released by proteolytic cleavage of APP, the β-peptide may exist in solution as either a random coil or an α-helical structure, which are both monomeric and very soluble. At physiological pH, the α-helices can associate to produce tetramers (Barrow et al., 1992; Zagorski & Barrow, 1992). The structural similarities with melittin and alamethicin suggest that a tetrameric assembly of α-helices for β-peptide may constitute its ion channel (Arispe et al., 1993a,b). We previously postulated that an α-helix→β-sheet conversion occurs for β-peptide during amyloid formation in AD, and this pathway may be mediated by the tetramer. At midrange pH, five positively charged and six negatively charged residues would reside on opposite faces of the helix, and this charge configuration could account for the helical association that occurs. Related α-helix (soluble, membrane-bound)→β-sheet (insoluble, aqueous solution) conversions of other peptides

and proteins, including the scrapie prion proteins, are well-known (Gasset et al., 1992; Hemminga et al., 1992; Pan et al., 1993).

Many theories about amyloid deposition in AD support the notion that local environmental factors in the human brain promote the precipitation of β-peptide from a soluble, nontoxic form to an insoluble, toxic form. In the amyloid plaque, the β-peptide exists in an oligomeric β-pleated-sheet structure that is resistant to further proteolysis and turnover (Crowther, 1991). One environmental factor is thought to be the binding of HSPG to β-peptide, as discussed above. In addition, the observation of the α-helical structure for β-peptide in membranelike environments can account for some of the features during β-amyloidosis. It is thought that amyloid deposition occurs in stages, where initially the more soluble and nontoxic pre-amyloid deposits (Yamaguchi et al., 1988; Joachim et al., 1989; Li et al., 1994) form prior to the insoluble, toxic amyloid plaques. In pre-amyloid deposits, β-peptide exists in an unpolymerized state (Frangione et al., 1993) and is not stained by cross β-pleated-sheet specific dyes such as Congo red and thioflavin-S (Mann, 1989). These facts, together with the knowledge that numerous membranelike components are present in pre-amyloid deposits (Masliah et al., 1991; Li et al., 1994), are consistent with an α-helical structure for β-peptide in pre-amyloid deposits. Further investigations concerning the structure and possible ion-channeling activity of pre-amyloid deposits are currently underway.

ACKNOWLEDGMENT

We thank Edmond L. Wang, Axel Brünger, Hoa Ton-That, Steve Younkin, Robert Friedland, Charles Sanders, Valerie Daggett, and Lawrence Sayre for many helpful discussions. We are also extremely grateful to Colin Barrow for the peptide synthesis. The NMR data were acquired using spectrometers located at the Suntory Institute for Bioorganic Research in Osaka, Japan, and at the Regional NMR Facility at the University of Wisconsin—Madison. The structural coordinates will be deposited in the Brookhaven Protein Data Base.

REFERENCES

Allsop, D., Wong, C. W., Ikeda, S.-I., Landon, M., Kidd, M., & Glenner, G. G. (1988) *Proc. Natl. Acad. Sci. U.S.A. 85*, 2790–2794.

Arispe, N., Rojas, E., & Pollard, H. B. (1993a) *Proc. Natl. Acad. Sci. U.S.A. 90*, 567–571.

Arispe, N., Pollard, H. B., & Rojas, E. (1993b) *Proc. Natl. Acad. Sci. U.S.A. 90*, 10573–10577.

Barany, M., Chang, Y.-C., Arus, C., Rustan, T., & Frey, W. H., II (1985) *Lancet i*, 517.

Barlow, D. J., & Thornton, J. M. (1988) *J. Mol. Biol. 201*, 601–619.

Barrow, C. J., & Zagorski, M. G. (1991) *Science 253*, 179–182.

Barrow, C. J., Yasuda, A., Kenny, P. T. M., & Zagorski, M. G. (1992) *J. Mol. Biol. 225*, 1075–1093.

Bazzo, R., Tappin, M. J., Pastore, A., Harvey, T. S., Carver, J. A., & Campbell, I. D. (1988) *Eur. J. Biochem. 173*, 139–146.

Blanco, F. J., Herranz, J., González, C., Angeles Jiménez, M., Rico, M., Santoro, J., & Nieto, J. L. (1992) *J. Am. Chem. Soc. 114*, 9676–9677.

Blusztajn, J. K., Gonzalez-Coviella, I. L., Logue, M., Growdon, J. H., & Wurtman, R. J. (1990) *Brain Res. 536*, 240–244.

Brunden, K. R., Richter-Cook, N. J., Chaturvedi, N., & Frederickson, R. C. A. (1993) *J. Neurochem. 61*, 2147–2154.

Brünger, A. T., & Nilges, M. (1993) *Q. Rev. Biophys. 26*, 49–125.

Burdick, D., Soreghan, B., Kwon, M., Kosmoski, J., Knauer, M., Henschen, A., Yates, J., Cotman, C., & Glabe, C. (1992) *J. Biol. Chem. 267*, 546–554.

Busciglio, J., Gabuzda, D. H., Matsudaira, P., & Yanker, B. A. (1993) *Proc. Natl. Acad. Sci. U.S.A. 90*, 2092–2096.

Chauhan, A., Chauhan, V. P. S., Brockerhoff, H., & Wisniewski, H. M. (1993) in *Alzheimer's Disease: Adavnces in Clinical and Basic Research* (Corain, B., Iqbal, K., Nicolini, M., Winblad, B., Wisniewski, H., & Zatta, P., Eds.) pp 431–439, Wiley, New York.

Cotman, C. W., Bridges, R., Pike, C., Kesslak, P., Loo, D., & Copani, A. (1993) in *Alzheimer's Disease: Adavnces in Clinical and Basic Research* (Corain, B., Iqbal, K., Nicolini, M., Winblad, B., Wisniewski, H., & Zatta, P., Eds.) pp 281–298, Wiley, New York.

Crowther, R. A. (1991) *Biochim. Biophys. Acta 1096*, 1–9.

Dempsey, C. E. (1990) *Biochim. Biophys. Acta 1031*, 143–161.

Dyson, H. J., & Wright, P. E. (1991) *Annu. Rev. Biophys. Chem. 20*, 519–538.

Dyson, H. J., & Wright, P. E. (1993) *Curr. Opin. Struct. Biol. 3*, 60–65.

Dyson, H. J., Merutka, G., Waltho, J. P., Lerner, R. A., & Wright, P. E. (1992a) *J. Mol. Biol. 226*, 795–817.

Dyson, H. J., Sayre, J., Merutka, G., Shin, H.-C., Lerner, R. A., & Wright, P. E. (1992b) *J. Mol. Biol. 226*, 819–835.

Dykstra, R. (1987) *J. Magn. Reson. 72*, 162–167.

Eckert, A., Hartmann, H., & Müller, W. E. (1993) *FEBS Lett. 330*, 49–52.

Esch, F., Keim, P. S., Beattle, E. C., Blacher, R. W., Culwell, A. R., Oltersdorf, T., McClure, D., & Ward, P. J. (1990) *Science 248*, 1122–1124.

Etcheberrigaray, R., Ito, E., Oka, K., Tofel-Grehl, B., Gibson, G. E., & Alkon, D. L. (1993) *Proc. Natl. Acad. Sci. U.S.A. 90*, 8209–8213.

Flood, J. F., Morley, J. E., & Roberts, E. (1991) *Proc. Natl. Acad. Sci. U.S.A. 88*, 3363–3366.

Fox, R. O., & Richards, F. M. *Nature 300*, 325–330.

Frangione, B., Wisniewski, T., Tagliavini, F., Bugiani, O., & Ghiso, J. (1993) in *Alzheimer's Disease: Adavnces in Clinical and Basic Research* (Corain, B., Iqbal, K., Nicolini, M., Winblad, B., Wisniewski, H., & Zatta, P., Eds.) pp 387–396, Wiley, New York.

Fraser, P. E., Nguyen, J. T., Surewicz, W. K., & Kirschner, D. A. (1991) *Biophys. J. 60*, 1190–1201.

Fraser, P. E., Nguyen, J. T., Chin, D. T., & Kirschner, D. A. (1992) *J. Neurochem. 59*, 1531–1540.

Frautschy, S. A., Baird, A., & Cole, G. M. (1991) *Proc. Natl. Acad. Sci. U.S.A. 88*, 8362–8366.

Gasset, M., Baldwin, M. A., Lloyd, D. H., Gabriel, J.-M., Holtzman, D. M., Cohen, F., Fletterick, R., & Prusiner, S. B. (1992) *Proc. Natl. Acad. Sci. U.S.A. 89*, 10940–10944.

Glenner, G. G., & Wong, C. W. (1984) *Biochem. Biophys. Res. Commun. 120*, 885–890.

Golde, T. E., Estus, S., Younkin, L. H., Selkoe, D. J., & Younkin, S. G. (1992) *Science 255*, 728–730.

Gorevic, P. D., Castano, E. M., Sarma, R., & Frangione, B. (1987) *Biochem. Biophys. Res. Commun. 147*, 854–862.

Haass, C., Schlossmacher, M. G., Hung, A. Y., Vigo-Pelfrey, C., Mellon, A., Ostaszewski, B. L., Lieberburg, I., Koo, E. H., Schenk, D., Teplow, D. B., & Selkoe, D. J. (1992) *Nature 359*, 322–325.

Hall, J. E., Vodyanoy, I., Balasubramanian, T. M., & Marshall, G. R. (1984) *Biophys. J. 45*, 233–247.

Halverson, K., Fraser, P. E., Kirschner, D. A., & Lansbury, P. T., Jr. (1990) *Biochemistry 29*, 2639–2644.

Havel, T. F. (1991) *Prog. Biophys. Mol. Biol. 56*, 43–78.

Hemminga, M. A., Sanders, J. C., & Spruijt, R. B. (1992) *Prog. Lipid Res. 31*, 301–333.

Hilbich, C., Kisters-Woike, B., Reed, J., Masters, C. L., & Beyreuther, K. (1991) *J. Mol. Biol. 218*, 149–163.

Ikura, T., Go, N., & Inagaki, F. (1991) *Proteins 9*, 81–89.

Jeener, J., Meier, B. H., Bachmann, P., & Ernst, R. R. (1979) *J. Chem. Phys. 71*, 4546–4553.
Joachim, C. L., Morris, J. H., & Selkoe, D. J. (1989) *Am. J. Pathol. 135*, 309–319.
Johnstone, E. M., Chaney, M. O., Norris, F. H., Pascual, R., & Little, S. P. (1991) *Mol. Brain Res. 10*, 299–305.
Kirschner, D. A., Inouye, H., Duffy, L. K., Sinclair, A., Lind, M., & Selkoe, D. J. (1987) *Proc. Natl. Acad. Sci. U.S.A. 84*, 6953–6957.
Kowall, N. W., Beal, M. F., Busciglio, J., Duffy, L. K., & Yanker, B. A. (1991) *Proc. Natl. Acad. Sci. U.S.A. 88*, 7247–7251.
Kuszewski, J., Nilges, M., & Brünger, A. T. (1992) *J. Biomol. Nucl. Magn. Reson. 2*, 33–56.
Lansbury, P. T., Jr. (1992) *Biochemistry 31*, 6865–6870.
Li, Y.-T., Woodruff-Pak, D. S., & Trojanowski, J. Q. (1994) *Neurobiol. Aging 15*, 1–9.
Mammi, S., Mammi, N. J., & Peggion, E. (1988) *Biochemistry 27*, 1374–1379.
Mancardi, G. L., Perdilli, F., Rivano, C., Leonardi, A., & Bugiani, O. (1980) *Acta Neuropathol. 49*, 79–83.
Mann, D. M. A. (1989) *Neurobiol. Aging 10*, 397–399.
Masliah, E., Cole, G. M., Hansen, L. A., Mallory, M., Albright, T., Terry, R. D., & Saitoh, T. (1991) *J. Neurosci. 11*, 2759–2767.
Masters, C. L., Simms, G., Weinman, N. A., Multhaup, G., McDonald, B. L., & Beyreuther, K. (1985) *Proc. Natl. Acad. Sci. U.S.A. 82*, 4245–4249.
Mattson, M. P., Tomaselli, K. J., & Rydel, R. E. (1993) *Brain Res. 621*, 35–49.
McDonnell, P. A., & Opella, S. J. (1993) *J. Magn. Reson., Ser. B 102*, 120–125.
Merutka, G., Morikis, D., Brüschweiler, R., & Wright, P. E. (1993) *Biochemistry 32*, 13089–13097.
Miyakawa, T., Shimoji, A., Kuramoto, R., & Higuchi, Y. (1982) *Virchows Arch. Cell Pathol. 40*, 121–129.
Namba, Y., Tomonaga, M., Kawasaki, H., Otomo, E., & Ikeda, K. (1991) *Brain Res. 541*, 163–166.
Nelson, J. W., & Kallenbach, N. R. (1986) *Proteins: Struct. Funct. Genet. 1*, 211–217.
Nilges, M., Clore, G. M., & Gronenborn, A. M. (1988) *FEBS Lett. 229*, 317–324.
Nitsch, R. M., Blusztajn, J. K., Pittas, A., Slack, B. E., Growdon, J. H., & Wurtman, R. J. (1992) *Proc. Natl. Acad. Sci. U.S.A. 89*, 1671–1675.
Otting, G., Widmer, H., Wagner, G., & Wüthrich, K. (1986) *J. Magn. Reson. 66*, 187–193.
Otvos, L., Jr., Szendrei, G. I., Lee, V. M.-Y., & Mantsch, H. H. (1993) *Eur. J. Biochem. 211*, 249–257.
Pan, K.-M., Baldwin, M., Nguyen, J., Gasset, M., Serban, A., Groth, D., Mehlhorn, I., Huang, Z., Fletterick, R. J., Cohen, F. E., & Prusiner, S. B. (1993) *Proc. Natl. Acad. Sci. U.S.A. 90*, 10962–10966.
Pardi, A., Billeter, M., & Wüthrich, K. (1984) *J. Mol. Biol. 180*, 741–751.
Parker, W., & Song, P.-S. (1992) *Biophys. J. 61*, 1435–1439.
Pettegrew, J. W., Panchalingam, K., Moossy, J., Martinez, J., Rao, G., & Boller, F. (1988) *Arch. Neurol. 45*, 1093–1096.
Pike, C. J., Walencewicz, A. J., Glabe, C. G., & Cotman, C. W. (1991) *Brain Res. 563*, 311–314.
Pike, C. J., Burdick, D., Walencewicz, A. J., Glabe, C. G., & Cotman, C. W. (1993) *J. Neurosci. 13*, 1676–1687.
Powers, R., Clore, G. M., Garrett, D. S., & Gronenborn, A. M. (1993) *J. Magn. Reson. 101*, 325–327.
Roher, A. E., Lowenson, J. D., Clarke, S., Wolkow, C., Wang, R., Cotter, R. J., Reardon, I. M., Zürcher-Neely, H. A., Heinrikson, R. L., Ball, M. J., & Greenberg, B. D. (1993) *J. Biol. Chem. 268*, 3072–3083.
Sansom, M. S. P. (1991) *Prog. Biophys. Mol. Biol. 55*, 139–235.
Schwarzman, A. L., Gregori, L., Vitek, M., Ljubski, S., Strittmatter, W. J., Englid, J., Bhasin, R., Silverman, J., Weisgraber, K. H., Cole, P., Zagorski, M. G., Talafous, J., Eizenberg, M., Saunders, A., Roses, A. D., & Goldgaber, D. (1994) *Proc. Natl. Acad. Sci. U.S.A.* (in press).
Segawa, S.-I., Fukuno, T., Fujiwara, K., & Noda, Y. (1991) *Biopolymers 31*, 497–509.
Selkoe, D. J. (1991) *Neuron 6*, 487–498.
Seubert, P., Vigo-Pelfrey, C., Esch, F., Lee, M., Dovey, H., Davis, D., Sinha, S., Schlossmacher, M., Whaley, J., Swindlehurst, C., McCormack, R., Wolfert, R., Selkoe, D. J., Lieberburg, I., & Schenk, D. (1992) *Nature 359*, 325–327.
Shoji, M., Golde, T. E., Ghiso, J., Cheung, T. T., Estus, S., Shaffer, L. M., Cai, X.-D., McKay, D., Tintner, R., Frangione, B., & Younkin, S. G. (1992) *Science 258*, 126–129.
Simmons, L. K., May, P. C., Tomaselli, K. J., Rydel, R. E., Fuson, K. S., Brigham, E. F., Wright, S., Lieberburg, I., Becker, G. W., Brems, D. N., & Li, W. (1993) *Soc. Neurosci. Abstr. 19*, Part 1, 397.
Sisodia, S. S. (1992) *Proc. Natl. Acad. Sci. U.S.A. 89*, 6075–6079.
Snow, A. D., Kinsella, M. G., Sekiguchi, R. T., Nochlin, D., & Wight, T. N. (1991) *Soc. Neurosci. Abstr. 17*, 1106.
Sönnichsen, F. D., Van Eyk, J. E., Hodges, R. S., & Sykes, B. D. (1992) *Biochemistry 31*, 8790–8798.
States, D. J., Haberkorn, R. A., & Ruben, D. J. (1982) *J. Magn. Reson. 48*, 286–292.
Szilágyi, L., & Jardetzky, O. (1989) *J. Magn. Reson. 83*, 441–449.
Terwilliger, T. C., & Eisenberg, D. S. (1982) *J. Biol. Chem. 257*, 6010–6015.
Tomski, S. J., & Murphy, R. M. (1992) *Arch. Biochem. Biophys. 294*, 630–638.
Van Geet, A. L. (1970) *Anal. Chem. 42*, 679–680.
Waterhous, D. V., & Johnson, W. C., Jr. (1994) *Biochemistry 33*, 2121–2128.
Wishart, D. S., Sykes, B. D., & Richards, F. M. (1991) *J. Mol. Biol. 222*, 311–333.
Wu, C.-S. C., & Yang, J. T. (1981) *Mol. Cell. Biochem. 40*, 109–122.
Wüthrich, K. (1986) *NMR of Proteins and Nucleic Acids*, Wiley, New York.
Yamaguchi, H., Hirai, S., Morimatsu, M., Shoji, M., & Harigaya, Y. (1988) *Acta Neuropathol. 77*, 113–119.
Yamaguchi, H., Nakazato, Y., Hirai, S., Shoji, M., & Harigaya, Y. (1990) *Am. J. Pathol. 135*, 593–597.
Zagorski, M. G. (1992) *J. Magn. Reson. 99*, 403–407.
Zagorski, M. G., & Barrow, C. J. (1992) *Biochemistry 31*, 5621–5631.
Zubenko, G. S., Wusylko, M., Cohen, B. M., Boller, F., & Teply, I. (1987) *Science 238*, 539–542.